Overcoming Nonlocal Effects and Brillouin Threshold Limitations in Brillouin Optical Time-Domain Sensors
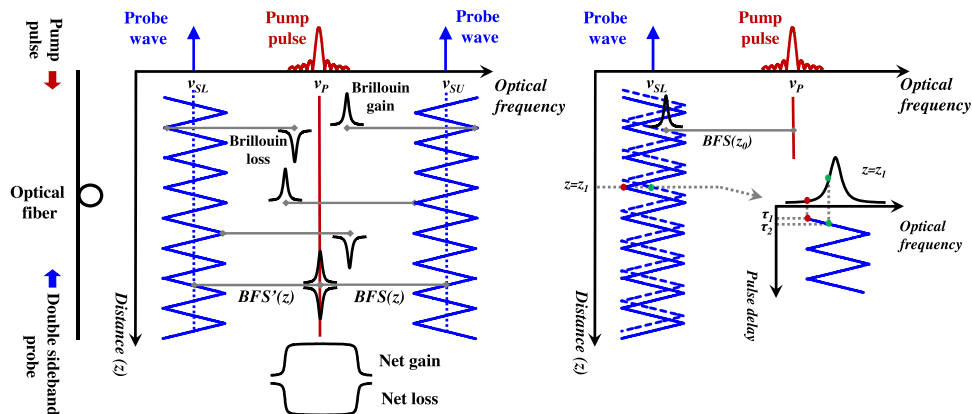
Rubén Ruiz-Lombera
Javier Urricelqui
Mikel Sagues, Member, IEEE
Jesús Mirapeix
José M. López-Higuera, Senior Member, IEEE
Alayn Loayssa, Member, IEEE

Overcoming Nonlocal Effects and Brillouin Threshold Limitations in Brillouin Optical Time-Domain Sensors

Rubén Ruiz-Lombera,[1] Javier Urricelqui,[2] Mikel Sagues,[2] *Member, IEEE*, Jesús Mirapeix,[1] José M. López-Higuera,[1] *Senior Member, IEEE*, and Alayn Loayssa,[2] *Member, IEEE*

[1]Photonics Engineering Group, Universidad de Cantabria, 39005 Santander, Spain
[2]Department of Electrical and Electronic Engineering, Universidad Pública de Navarra, 31006 Pamplona, Spain

Abstract: We demonstrate, for the first time to our knowledge, a Brillouin optical time-domain analysis (BOTDA) sensor that is able to operate with a probe power larger than the Brillouin threshold of the deployed sensing fiber and that is free from detrimental nonlocal effects. The technique is based on a dual-probe-sideband setup in which an optical frequency modulation of the probe waves along the fiber is introduced. This makes the optical frequency of the Brillouin interactions induced by each probe wave on the pump vary along the fiber so that two broadband Brillouin gain and loss spectra that perfectly compensate are created. As a consequence, the pulse spectral components remain undistorted, avoiding nonlocal effects. Therefore, very large probe power can be injected, which improves the signal-to-noise ratio (SNR) in detection for long-range BOTDA. Moreover, the probe power can even exceed the Brillouin threshold limit due to its frequency modulation, which reduces the effective amplification of spontaneous Brillouin scattering in the fiber. Experiments demonstrate the technique in a 50-km sensing link in which 8 dBm of probe power is injected.

Index Terms: Brillouin distributed sensors, Brillouin optical time-domain analysis, nonlocal effects, Brillouin threshold, optical fiber sensors, stimulated Brillouin scattering.

1. Introduction

Brillouin optical time-domain analysis (BOTDA) sensor technology has evolved over the past few years to such an extent that it has become a powerful tool to monitor temperature and strain over large structures. These measurement are of great value for diverse field applications, such as ensuring the structural health of oil and gas pipelines or assessing the operating conditions of high voltage transmission lines, all of which have a common need for large monitoring distances.

One of the main limitations to the deployment of such long-range BOTDAs comes from so-called non-local effects. These are due to the interaction of the two optical waves that counter-propagate

in a BOTDA: the pump pulse and the probe wave. BOTDA measurements are based on characterizing the gain spectra that the pump pulse provides to the probe wave at each position of the fiber. However, this gain comes from energy transfer that leads to the depletion of the pump pulse as it propagates along the sensing fiber. The larger the probe wave that is amplified, the larger the pump depletion. Moreover, the pump depletion depends on the optical frequency of the probe, which introduces a distortion in the measured Brillouin gain spectra and, hence, a systematic error in the measurement of the Brillouin frequency shift (BFS) [1]. Altogether, this results in a limit to the maximum probe power that can be launched into the fiber and hence a reduction in detection signal-to-noise ratio.

Several methods have been proposed to counteract this limitation [1]–[6]. For instance, the use of a BOTDA deploying phase modulation of the probe and RF phase-shift detection [3]. Also the use of different techniques that divide into several sections the entire sensing fiber to reduce the effective Brillouin amplification length so that the Brillouin interaction length only takes place in a portion of the fiber. Examples of this, are techniques based on frequency division multiplexing (FDM) [4], time division multiplexing (TDM) [5] or pulsing the probe wave [6]. Nevertheless, the most popular method to compensate this detrimental effect to date has been the use of a dual-probe-sideband setup, in which two sidebands equally spaced from the pulse wavelength provide a complementary interaction, such that the energy that the pulse transfers to the lower optical frequency probe is compensated by that transferred from the upper optical frequency probe to the pulse [1], [2]. However, it has been recently shown that the probe power that can be deployed in such dual-probe-sideband setup is rather limited, because non-local effects are compensated only to first order and there is an additional distortion of the pump pulse spectra that is brought by the combined gain and loss spectra generated by the two probe waves [7].

Therefore, the limitation to long-range BOTDAs coming from non-local effects is yet to be resolved. Furthermore, even though non-local effects were completely overcome, another limit for the probe power would remain: the Brillouin threshold of the fiber. This threshold defines the maximum power that can be launched into the sensing fiber before the amplification of thermally-induced spontaneous Brillouin scattering (SpBS) leads to depletion of the probe wave and addition of noise to the detected signal [8], [9].

In this work, we introduce a method to greatly expand the probe power that can be deployed in BOTDA sensors, overcoming previous non-local effect limits and even the Brillouin threshold limit. It is based on modulating the optical frequency of the probe waves in a dual-probe BOTDA setup. Moreover, this technique avoids the need to sweep the frequency of the probe waves by changing the microwave frequency applied to the modulator used to generate those waves. Instead, the Brillouin gain spectra are characterized by changing the delay between the pump pulse and the probe wave optical frequency modulation.

2. Description of the Technique

Fig. 1 shows the fundamentals of the technique by depicting the spectra of the various optical waves involved. A BOTDA setup with two probe waves counter-propagating to the pump pulse was assumed. As it is highlighted in the figure, the optical frequency of the probe waves is modulated in the time domain. Moreover, this FM signal is synchronized to the pump pulses so that a sequence of pulses experiences the same wavelength of the probe waves at any given location. Therefore, the modulation of the optical frequency of the probe waves leads to a variation of the Brillouin interaction frequency along the fiber that follows the same profile of this modulation.

This has important implications for the Brillouin interaction generated by both probe waves onto the pump pulse, as it is schematically depicted in Fig. 1(a). The modulation of the optical frequency of the probe waves makes the Brillouin interaction induced by them upon the optical pulse to spread over a large frequency range so that non-local effects cease to be significant. This can be understood by taking into account that the lower-frequency probe induces a loss
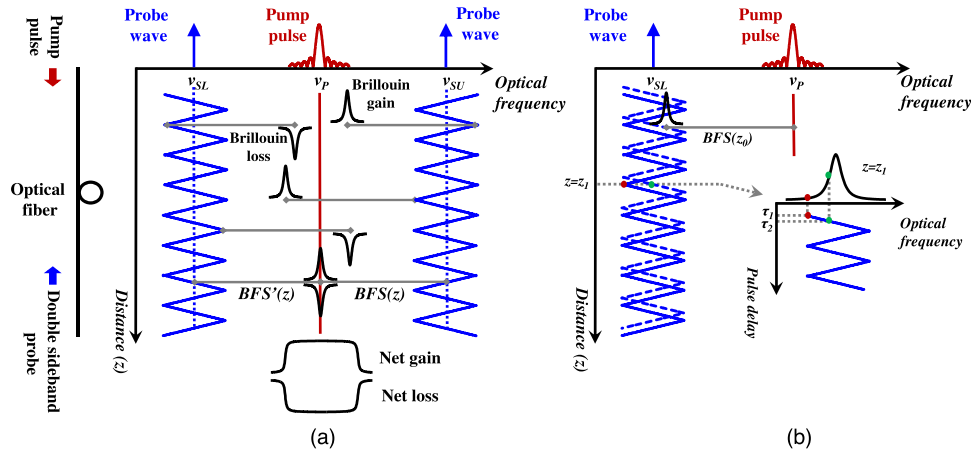
Fig. 1. Fundamentals of the technique: Details of the Brillouin interaction on the pump pulse (a) and on the probe wave (b).

spectrum to the pulse that changes its central frequency along the fiber. The interaction at a particular location is given by the detuning of the Brillouin loss spectra from the pulse $\Delta\nu_L$

$$\Delta\nu_L(z) = \nu_{SL}(z) - \nu_P(z) + \text{BFS}(z) \tag{1}$$

where ν_P and ν_{SL} are the optical frequencies of the pump pulse and the lower-frequency probe sideband, respectively. The change in ν_{SL} along the fiber mimics the shape of the FM modulation imposed on the probe wave. The integration of this loss interaction along the fiber gives a flat wideband total depletion spectrum that does not distort the pulse spectrum, provided that an adequate shape is chosen for the frequency modulation. Similarly, the upper-frequency probe wave induces a gain spectrum that has a variation along the fiber given its detuning from the pulse $\Delta\nu_G$

$$\Delta\nu_G(z) = \nu_P(z) - \nu_{SU}(z) + \text{BFS}(z) \tag{2}$$

where ν_{SU} is the optical frequency of the upper-frequency probe sideband. Again, integration of this along the fiber gives a flat wideband total gain spectrum that compensates the pulse depletion. Therefore, the gain and loss spectra perfectly compensate for all the frequency components of the pulse, and hence, non-local effects are fully avoided.

A triangular modulation of the probe waves frequency is assumed in Fig. 1. However, other modulation shapes are possible to optimize the objective of having the flattest possible total gain and depletion spectra so that no distortion is introduced to the pulse.

In detection, just one of the probe waves is detected, typically the lower frequency one, while the other is filtered out. In order to measure the Brillouin spectra experienced by the retained probe wave at any given location, it is necessary to scan the frequency of the probe wave at that location. In a conventional BOTDA this is done by sweeping the frequency of the probe wave. However, in our system this can be done in a much simpler way by sequentially changing the relative delay between the pump pulses and the FM wave, as it is schematically depicted in Fig. 1(b). This changes the relative location of the optical frequency profile of the probe wave along the fiber so that at any given location all frequencies are sequentially scanned.

This new technique of using FM modulation of the probe waves can be regarded as an evolution of our previous proposal to generate virtual BFS profiles along a sensing fiber [10]. However, in that case, the method was based on modulating the wavelength of the laser source used to generate the optical waves needed in a self-heterodyne BOTDA setup, rather than directly modulating the probe wave frequency. Moreover, in that previous work, the pulse
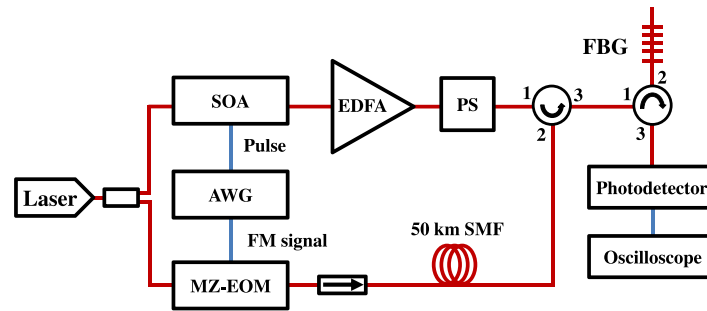
Fig. 2. Experimental setup.

depletion was not compensated but simply made flatter in terms of its frequency dependence to avoid BFS measurement errors.

3. Experimental Setup

Fig. 2 depicts the assembled setup used to demonstrate our technique. The output of a laser source is divided into two branches to generate the pump and probe waves. In the upper branch, the pump signal is pulsed using a semiconductor optical amplifier (SOA). Then, the pulse power is boosted to a peak of 140 mW using a erbium doped fiber amplifier (EDFA) and its polarization state is randomized using a polarization scrambler (PS) before being launched into 50 km of standard single-mode fiber (SMF).

In the lower branch, a double-sideband probe wave is generated using a Mach–Zehnder electro-optic modulator (MZ-EOM) driven by an arbitrary waveform generator (AWG) and biased at the minimum transmission point of its transfer curve. The AWG provides a FM microwave signal whose instantaneous frequency varies around the average BFS of the fiber following a triangular shape. This induces an identical modulation of the optical frequency of the probe waves. The microwave signal has been designed to have a carrier frequency of 10.8 GHz and a peak frequency deviation of 75 MHz. The modulation frequency is 40 KHz, which yields a total of 20 cycles of triangular variation of the local probe frequency along the 50 km long sensing fiber.

When the Brillouin interaction provided by such FM modulated probe waves is integrated along the fiber, it gives Brillouin gain and loss spectra with a bandwidth of around 150 MHz, which is more than enough to avoid distortion in 10-ns pulses for 1-m resolution. Shorter pulses can be accommodated simply by increasing the peak frequency deviation. In the particular proof-of-concept experiments described in this paper, 50-ns pulses are deployed.

Finally, after Brillouin interaction of these probe signals with the pump pulse, they are directed to a fiber Bragg grating (FBG) to filter out the upper sideband. The remaining probe wave is detected and captured in a digital oscilloscope and processed in a computer.

4. Experimental Results

We started our experiments by confirming that, indeed, in the conventional dual-probe BOTDA there is a serious problem with non-local effects as the probe power is increased. This is done by simply switching off the FM modulation on the AWG so that it generates tunable CW micro-wave tones and sweeping the optical frequency of the probe waves to scan the Brillouin spectra along the fiber.

Fig. 3(a) and (c) show the pulses that are measured at the output of the fiber as the micro-wave frequency is swept to measure the Brillouin spectra for two cases with low probe power (−6 dBm) and with high probe power (5 dBm). Notice that when the probe power is low, non-local effects are negligible so the pulse remains constant and undistorted for all the probe's optical frequencies. However, when the probe power is increased the pulses are greatly distorted depending on the probe frequency. This distortion has been previously reported in the literature, but the effect
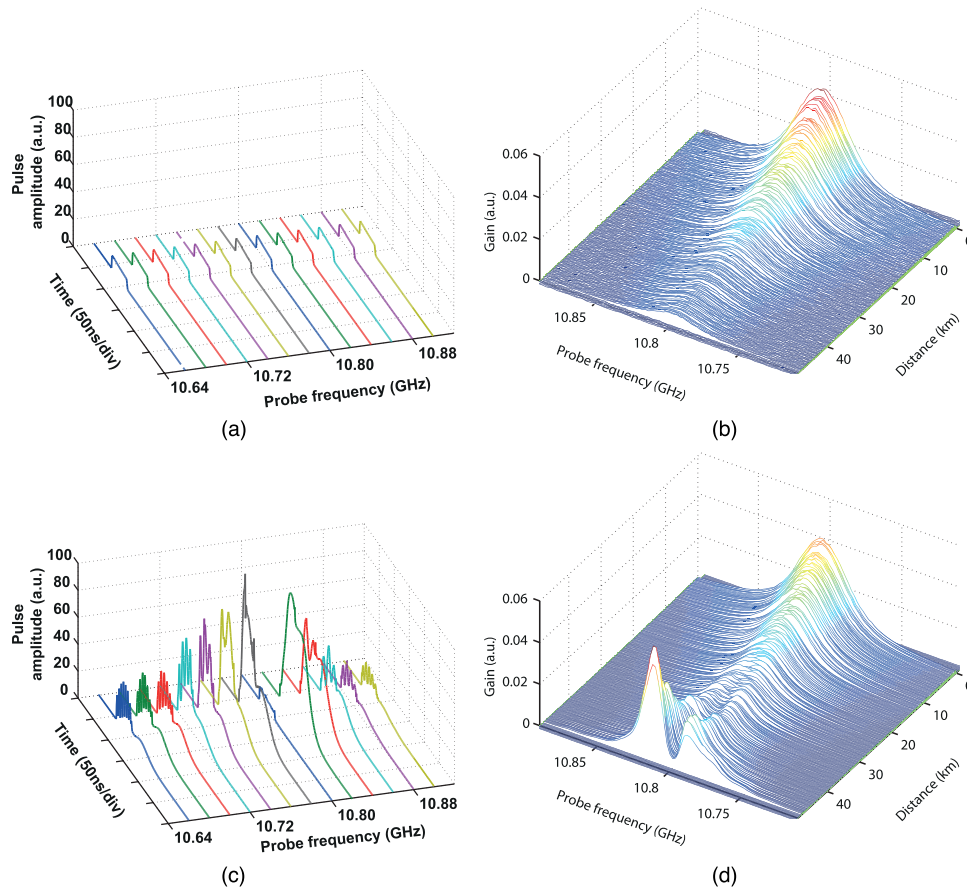
Fig. 3. Pulses at the output of the fiber and measured Brillouin spectra for a conventional dual-probe BOTDA in two cases for probe wave powers of −6 dBm (a), (b) and 5 dBm (c), (d).

was found to be rather mild due to the deployment of lower probe powers than the one used here [7]. However, it can be seen that the distortion is much more pronounced as the probe wave power is increased. In Fig. 3(c), it can be seen that the gain and depletion induced by both probe waves upon the pulse compensate just when the microwave frequency coincides with average BFS of the fiber (around 10.8 GHz). However, for small departures of the microwave frequency from that value, the pulse gets distorted as its spectral components get differential amplification or depletion [7]. This makes the pulse peak power to greatly increase around the BFS frequency. There is also increased temporal duration of the pulses at those frequencies.

The distortion of the pulses has a strong impact on the measured Brillouin spectra along the fiber. Fig. 3(b) and (d) show a 3-D view of the Brillouin spectra measured for the two cases considered before. It is clearly appreciated that for larger probe powers at the far away locations of the fiber, where the pulse arrives with great distortion, the measured spectra are also greatly distorted. Note that in Fig. 3(d), the spectra at the end of the fiber have two peaks around the mean BFS of the fiber that correspond to the probe frequencies at which the pulse is shown to be amplified in Fig. 3(c).

A more detailed view of the spectra at the end of the fiber is highlighted in Fig. 4. It shows how the spectra are affected by the distortion of the pulse spectra due to non-local effects when the probe power is increased. These spectra have lost his Lorentzian shape and two peaks have appeared around its center due to the amplification of the pulse at those frequencies.

In contrast to the conventional technique, Fig. 5 depicts measurements with our technique with FM modulation of the probe waves. Fig. 5(a) depicts the pulses measured at the output of the fiber with and without probe wave applied. Notice that the pulse shape remains almost
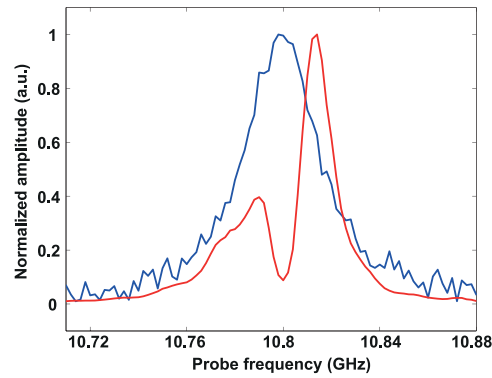
Fig. 4. Measured Brillouin spectra at the end of the fiber for −6 dBm (blue line) and 5 dBm (red line) probe power.
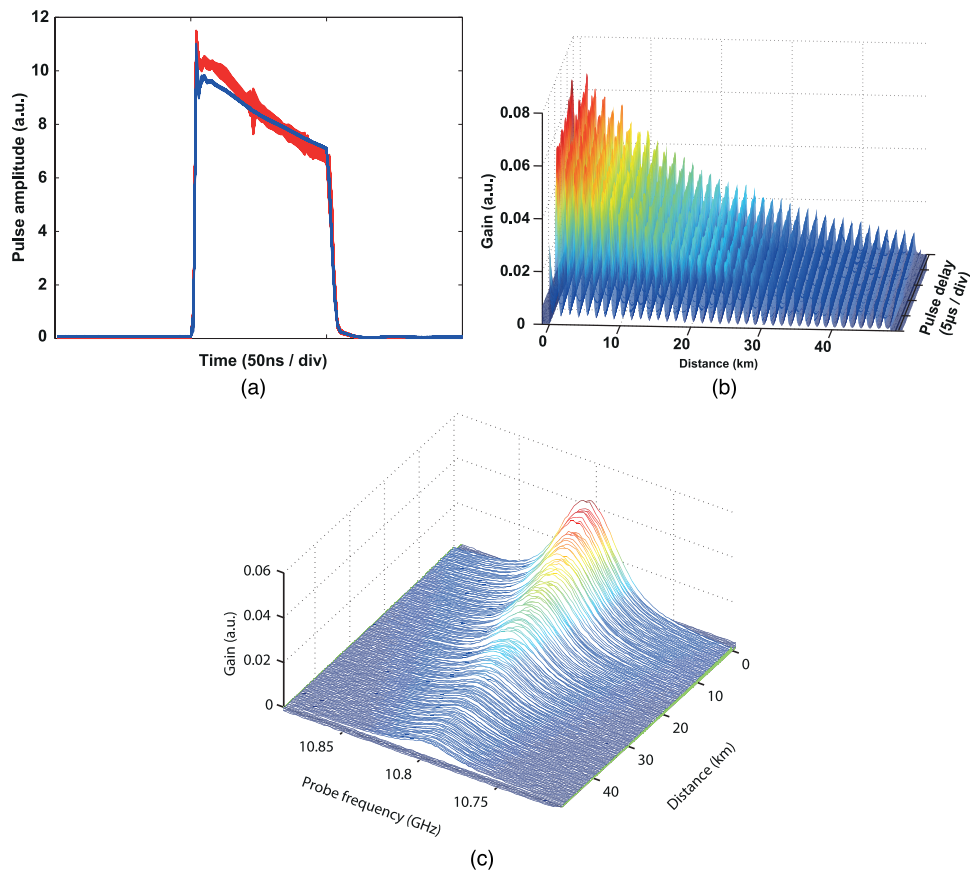

Fig. 5. (a) Pulses at the output of the fiber in two cases for probe wave power of 8 dBm (red line) and without probe power (blue line). (b) Raw measurement data for the FM dual-probe BOTDA with 8 dBm probe power and (c) measured Brillouin spectra.

identical for both cases with negligible distortion and just some added noise, which is attributed to SpBS amplified by the probe waves. In addition, note that the deployed probe power is larger than for previous measurements, i.e., 8 dBm, which, to our knowledge, is the largest probe power ever demonstrated in a long-range BOTDA sensor without errors induced by non-local effects. The raw measurement data, obtained as the delay between the pulse and the FM
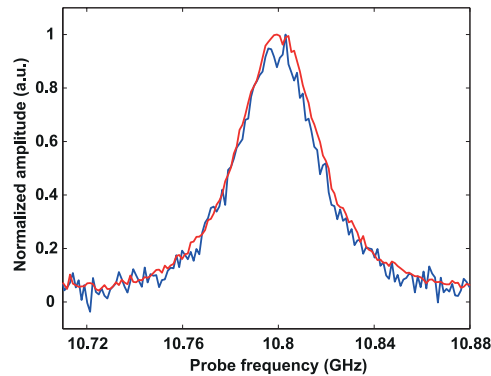
Fig. 6. Measured Brillouin spectra at the end of the fiber for −6 dBm (blue line) and 8 dBm (red line) probe powers with the FM dual-probe BOTDA system.
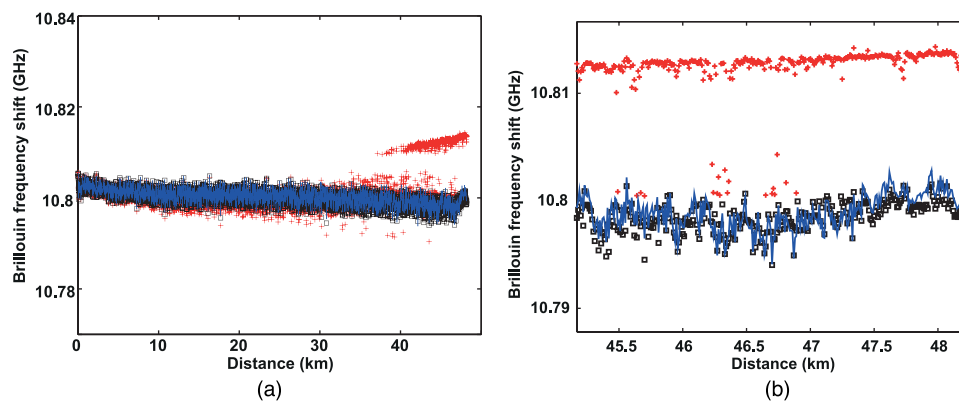

Fig. 7. Comparison of measured BFS for the FM technique with 8 dBm probe power (blue solid line) and for the conventional dual probe with 5 dBm (red crosses) and −6 dBm (black squares) probe power for (a) all the fiber and (b) in the last few kilometers.

modulation is modified, is depicted in Fig. 5(b). Note that it follows the shape of the FM modulating signal. This raw data is post-processed to compensate the frequency shift in the measurement introduced by FM modulation of the probe wave along the fiber. With this purpose, at each location z, the frequencies in the measured spectra are reordered to account for the delay changes that are introduced between the pulses and the FM signal during the measurement process, as it was explained in Fig. 1(b). This is a simple and immediate operation that does not introduce any significant calculation delay, resulting in the measurement of the well-behaved spectra in Fig. 5(c). The spectra are completely normal, not suffering any distortion at the end of the fiber.

Fig. 6 compares the spectra measured at the output of the fiber for our FM technique with low and high powers of the probe wave. It can be seen that, indeed, the larger power measurement is not distorted at all. The only difference between the measurements is that the higher power one is significantly less noisy, as it was expected, due to the higher probe wave reaching the receiver. Moreover, there is no systematic error in the BFS measurement given by both spectra. Note that the full potential improvement in signal-to-noise ratio (SNR) generated with the presented technique is limited, for this particular case, by the maximum optical power injected to the receiver (−13 dBm).

Therefore, with our technique there is no systematic error in the BFS measurement when the probe power is increased. This is confirmed by Fig. 7 that displays the BFS measured for the conventional dual-probe BOTDA and for our system for different powers of the probe wave. Notice that, as it was explained before, there is a large systematic measurement error as the probe
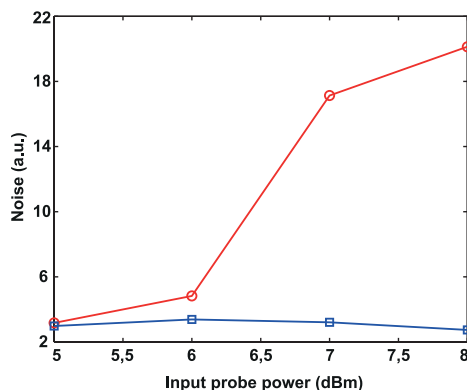
Fig. 8. Comparison of measured rms noise at the detector for different probe powers injected in the fiber using the conventional dual probe system (red line with circles) and the FM technique (blue line with squares).

power is increased for the conventional dual-probe BOTDA, while for our system, the BFS measurement remains error-free, even for larger probe power.

Finally, it must be pointed out that our FM BOTDA setup is operating with a probe power above the Brillouin threshold, which was measured to be 6-dBm for the deployed sensing fiber. This is made possible by a side effect of the FM modulation, which has been previously shown to increase the effective Brillouin threshold [11]. This is confirmed by measuring the rms noise at the detector for different probe power injected in the fiber but using an attenuator to keep a constant received power. As is shown in Fig. 8, in the conventional dual probe system there is a larger than six times increment in rms noise as the probe power is increased from 5 dBm to 8 dBm, whereas with the FM technique the noise level remains stable. This is confirmed by measuring the rms noise at the detector for different probe power injected in the fiber but using an attenuator to keep a constant received power. As is shown in Fig. 8, in the conventional dual probe system there is a larger-than-six times increment in rms noise as the probe power is increased from 5 dBm to 8 dBm, whereas with the FM technique the noise level remains stable.

5. Conclusion

In this paper, we have introduced a new technique for dual-probe-sideband BOTDA sensors based on deploying FM modulation of the probe waves. The experiments have demonstrated that this method permits much more power injected in the sensing fiber than was previously possible, opening the way to a substantial enhancement in the performance of BOTDA sensors. This will come in the form of enhanced SNR in the detectors at the end of the fiber as more optical power reaches them, which, in turn, leads to enhanced sensor performance in terms of precision or measurement time.

References

[1] L. Thévenaz, S. Mafang, and J. Lin, "Effect of pulse depletion in a Brillouin optical time-domain analysis system," *Opt. Exp.*, vol. 21, no. 12, pp. 14017–14035, 2013.

[2] A. Minardo, R. Bernini, and L. Zeni, "A simple technique for reducing pump depletion in long-range distributed Brillouin fiber sensors," *IEEE Sensors J.*, vol. 9, no. 6, pp. 633–634, Jun. 2009.

[3] J. Urricelqui, M. Sagues, and A. Loayssa, "BOTDA measurements tolerant to non-local effects by using a phase-modulated probe wave and RF demodulation," *Opt. Exp.*, vol. 21, no. 14, pp. 17186–17194, Jul. 2013. [Online]. Available: http://www.opticsexpress.org/abstract.cfm?URI=oe-21-14-17186

[4] Y. Dong, L. Chen, and X. Bao, "Extending the sensing range of Brillouin optical time-domain analysis combining frequency-division multiplexing and in-line EDFAS," *J. Lightw. Technol.*, vol. 30, no. 8, pp. 1161–1167, Apr. 2012.

[5] Y. Dong, L. Chen, and X. Bao, "Time-division multiplexing-based BOTDA over 100 km sensing length," *Opt. Lett.*, vol. 36, no. 2, pp. 277–279, Jan. 2011.

 [6] A. Zornoza, A. Minardo, R. Bernini, A. Loayssa, and L. Zeni, "Pulsing the probe wave to reduce nonlocal effects in Brillouin optical time-domain analysis (BOTDA) sensors," *IEEE Sensors J.*, vol. 11, no. 4, pp. 1067–1068, Apr. 2011.

 [7] A. Domínguez-López, X. Angulo-Vinuesa, A. López-Gil, S. Martín-López, and M. González-Herráez, "Non-local effects in dual-probe-sideband Brillouin optical time domain analysis," *Opt. Exp.*, vol. 23, no. 8, pp. 10341–10352, Apr. 2015. [Online]. Available: http://www.opticsexpress.org/abstract.cfm?URI=oe-23-8-10341

 [8] T. Shimizu, K. Nakajima, K. Shiraki, K. Ieda, and I. Sankawa, "Evaluation methods and requirements for the stimulated Brillouin scattering threshold in a single-mode fiber," *Opt. Fiber Technol.*, vol. 14, no. 1, pp. 10–15, Jan. 2008.

 [9] A. David and M. Horowitz, "Low-frequency transmitted intensity noise induced by stimulated Brillouin scattering in optical fibers," *Opt. Exp.*, vol. 19, no. 12, pp. 11792–11803, Jun. 2011.

[10] J. Urricelqui, M. Sagues, and A. Loayssa, "Synthesis of Brillouin frequency shift profiles to compensate non-local effects and Brillouin induced noise in BOTDA sensors," *Opt. Exp.*, vol. 22, no. 15, pp. 18195–18202, Jul. 2014.

[11] J. B. Coles *et al.*, "Bandwidth-efficient phase modulation techniques for stimulated Brillouin scattering suppression in fiber optic parametric amplifiers," *Opt. Exp.*, vol. 18, no. 17, p. 18138, Aug. 2010.